

**Internal transitions of quasi-2D charged magneto-excitons in the presence of weak lateral
confining potentials**

C. J. Meining, V. R. Whiteside, B. D. McCombe

Department of Physics and CSEQuIN, University at Buffalo, SUNY, Buffalo, NY 14260, USA

A. B. Dzyubenko*

Department of Physics, CSU at Bakersfield, CA 93311, USA

J. G. Tischler, A. S. Bracker, D. Gammon

Naval Research Laboratory, Washington, D.C. 20375-5347, USA

Abstract

Optically detected resonance spectroscopy has been used to investigate effects of weak random lateral potential fluctuations on internal transitions of charged magneto-excitons in quasi two-dimensional GaAs/AlGaAs quantum well (QW) systems. Resonant changes in the ensemble photoluminescence induced by far-infrared radiation were studied as a function of magnetic field for 1) samples with nominally smooth QW interfaces, and 2) samples with intentional growth interrupts, which lead to long range monolayer differences of QW width and concomitant variations in the lateral potential. While only bound-to-continuum internal transitions were observed in the first case, a feature seen on the high field (low energy) side of electron cyclotron resonance in the latter case for wider wells is attributed to a bound-to-bound transition of the spin-triplet state, with finite oscillator strength due to breaking of translational symmetry.

PACS number(s): 71.35.Pq, 71.70.Di, 73.21.-b, 76.40.+b

Internal transitions of neutral and charged excitons depend strongly on the symmetry properties of these electron-hole complexes in quasi-two-dimensional (2D) GaAs/AlGaAs quantum wells (QWs) in an applied magnetic field. As an example, for the neutral quasi-2D exciton (X), the axial symmetry of the Coulomb bound electron-hole pair in a magnetic field results in a direct relationship between the energies of excited, low-field p-like states of the X and electron/hole single particle cyclotron energies. This result is independent of magnetic field and holds even for the complex valence band Landau level (LL) structure of a QW, where heavy-hole and light-hole levels strongly interact provided the warping terms are weak.^{1,2} With an additional electron bound to a single hole, i.e., for a negatively charged exciton (X⁻), a symmetry related to the center-of-mass (CM) motion leads to surprisingly strict selection rules and becomes apparent in magneto-optics.^{3,4} In contrast to the superficially similar negatively charged donor D⁻,^{5,6} the positive charge of an X⁻-complex is mobile and free to move in the QW plane. As a consequence, internal bound-to-bound transitions are forbidden and only bound-to-continuum transitions are allowed for the X⁻.^{3,4} When the magnetic translational symmetry of the X⁻-complex is broken, the forbidden bound-to-bound transitions become allowed, and acquire a finite oscillator strength.^{3,7}

In this work we report effects of purposefully introduced, weak random lateral potentials due to monolayer (ML) interface fluctuations on internal transitions of X⁻. The consequences of symmetry breaking are shown directly by optically detected resonance (ODR) spectroscopy. In this highly sensitive technique⁸ internal transitions from the ground state associated with the lowest electron Landau level ($n_e = 0$) to excited states associated with the first excited Landau level ($n_e = 1$) can be observed by monitoring resonant changes of the (ensemble) photoluminescence (PL) induced by absorption of a far-infrared (FIR) laser beam in a magnetic

field. We compare data for a QW with nominally smooth interfaces (lateral range of fluctuations small on the scale of the exciton Bohr radius) and a QW for which lateral fluctuations of the (QW) width with lateral scales of several Bohr radii have been purposefully introduced by interrupting the epitaxial growth at the interface. To our knowledge, electric-dipole-allowed intraband transitions have not been studied previously for samples having controlled interface fluctuations, (interface-fluctuation quantum dots, IFQDs^{9, 10}), although investigations of ensembles of self-assembled InAs/GaAs¹¹ and InSb/GaSb¹² quantum dots by ODR spectroscopy have recently been reported. In addition, these ODR measurements may provide insight into the various mechanisms that lead to breaking of translational invariance currently under debate. In particular, such studies may serve to clarify the elusive role of trion localization; a variety of behaviors, ranging from complete localization¹³ to charge transport by trions,¹⁴ has been reported for nominally very similar samples.

Two GaAs/AlGaAs QW samples grown by molecular beam epitaxy on semi-insulating GaAs (100) substrates were investigated. Sample 1 consists of 40 repetitions of 20 nm GaAs wells sandwiched between 40 nm Al_{0.3}Ga_{0.7}As barriers, δ -doped with silicon at $2 \times 10^{10} \text{ cm}^{-2}$. This sample was grown without growth interrupts at the QW interfaces and the length scale of the interfacial roughness is therefore expected to be much smaller than the exciton Bohr diameter.^{15, 16} Sample 2 contains five single QWs of nominal widths 2.8, 4.2, 6.2, 8.4 and 14.1 nm with the narrowest well closest to the sample surface;¹⁷ the QWs are separated by 40 nm Al_{0.3}Ga_{0.7}As barriers. After the growth of a particular well, the barrier, consisting of 10 nm of undoped AlGaAs followed by 3 nm of Si-doped AlGaAs at (10^{17} cm^{-3}) was grown, yielding an electron density close to that of sample 1. The growth was interrupted at the well/barrier interfaces to form monolayer high lateral islands, which serve as natural quantum dots in this

system¹⁸ for the narrower QWs. The importance of lateral localization of neutral and charged excitons has been demonstrated for such samples by the very narrow homogeneously broadened PL lines¹⁹ obtained from single dot studies of the narrowest wells. Here, we concentrate on the results of the (two) widest well(s), where single dot spectra are not obtained due to the small (< 1 meV) lateral confinement, but the random lateral fluctuating potential is manifest by its effects on the internal transitions and translational invariance. The ODR spectra of the narrower wells have been interpreted as an inhomogeneously broadened ensemble of internal transitions.¹⁰ ODR spectra for sample 1 were obtained with a fiber optic/far infrared light pipe setup,^{2, 8} while measurements on sample 2 were taken with focusing optics for both visible/near IR and far IR beams.¹⁰

Photoluminescence spectra of both samples show multiple features that were previously observed and identified^{17, 20} as recombination from neutral and negatively charged excitons. In the case of sample 2 additional “fine” structure is observed from the ML well-width fluctuations. The measured separation (MLS) of corresponding features (X or X⁻) due to one ML difference in well width is approximately 0.75 meV, in good agreement with a calculation of the lowest QW subband energies of finite barrier GaAs/Al_{0.3}Ga_{0.7}As QWs with typical parameters.²¹ The zero field trion binding energies for samples 1 and 2 are about 1.3 meV and 1.4 meV, respectively.

Figure 1(c) shows the PL at 6.24 T, the field corresponding to electron cyclotron resonance (eCR), with a resolution of about 0.8 meV (CCD detection), not sufficient to resolve the fine structure arising from ML well-width fluctuations. The PL is shown without (dashed line) and with (solid line) simultaneous FIR illumination ($P = 180$ mW) at $E_{\text{FIR}} = 10.43$ meV. At this FIR photon energy and magnetic field, electrons undergo cyclotron resonance transitions between the two lowest LLs (at this field at low temperatures essentially all electrons are in the

lowest Landau level) and resonantly heat the carrier system. As a result, the X^- population increases at the expense of the X^- population, which gives rise to a negative ODR signal (black hatched region) in Fig. 1(c) for the latter and a positive ODR signal (white hatched region) for the former. This process involves a combination of partial ionization of the photo-excited X^- -complexes and carrier redistribution in the laterally modulated potential landscape. Figure 1(a) shows a grayscale contour plot of the ODR signal strength as a function of PL energy and magnetic field ($\Delta B = 0.02$ T) obtained with CCD detection. Dark (bright) contours correspond to negative (positive) ODR signal, while grey indicates zero signal. The dotted vertical line marks eCR, for which a constant field ODR signal (the difference between FIR laser on and off) is shown by the dotted white line in Fig. 1(c). Note that the X^- (X) ODR signal remains negative (positive) over the entire field range, and that both features shift to higher energies with increasing field in accord with the diamagnetic shift of the excitonic complexes. The field dependence of the ODR signal can be obtained by tracking one of the PL features. The two black lines in Fig. 1(a) indicate the energy bandpass (0.6 meV) over which such a signal was obtained for the X^- feature; the result averaged over this bandpass is shown in Fig. 1(b) (thick black line). Similar results can be obtained with a combination of PMT and Lock-in detection while tracking the same feature with a spectral window set by the spectrometer slits and with the spectrometer drive programmed to follow the field dependence of the feature (thin white line in Fig. 1(b)). Note that one obtains inverted signals when tracking the neutral X feature. In both cases multiple resonances, labeled S_1 , S_2 , T_1 , and T_b , are observed in addition to eCR. These features are described in more detail below. The internal transitions of the X^- -singlet S_1 , S_2 , and the X^- -triplet T_1 (for high-field schematic of triplet states see inset of Fig. 2) occur at fields close to the previously observed and identified⁴ transitions in quantum wells without growth interrupts. They

correspond to ionizing transitions of an electron from a bound X^- -state associated with the lowest electron Landau level to the continuum of scattering states (hatched regions in the inset to Fig. 2) associated with the 2nd electron LL. In the high-field limit these can be thought of as CR-like transitions modified by the electron-electron and electron-hole Coulomb interactions³. In particular, transitions S_1 and T_1 (for the latter see inset to Fig. 2) correspond to CR-like transitions of the “second” electron in the X^- -complex in singlet and triplet states, respectively; the other two carriers of the complex, a neutral X , remain in their respective ground states. The transitions labeled S_2 and T_2 , on the other hand, correspond approximately to internal transitions of bound electron-hole pairs (X), from the ground singlet or triplet state to an excited p-like state with the “second” electron remaining in the lowest LL. The triplet transition T_2 occurs at much higher photon energies, i.e. lower magnetic fields, outside of the region probed by the experiment and is therefore not observed. These are the only electric-dipole-allowed transitions in 2D QW systems for which both axial symmetry (the angular momentum selection rule) and the magnetic translational invariance, are preserved.^{3, 7} High-accuracy numerical calculations show that as magnetic field decreases, more than two prominent peaks may develop in the singlet X^- transitions, while the picture of the two triplet transitions still remains qualitatively valid. We believe this happens because (i) the gap between scattering states belonging to different LL’s closes at low fields and (ii) the mixing of states in different LL’s due to electron-electron interactions is much stronger for the singlet X^- -states. In the high-field, strictly 2D limit, it can be shown^{3, 7} that a lateral potential, modeled by a harmonic oscillator potential, leads to translational symmetry breaking, and therefore the bound-to-bound triplet transition with its energy position below eCR and formerly forbidden by magnetic translational invariance, becomes allowed and acquires a finite oscillator strength, which depends on the strength of the

lateral potential. The random potential due to the interface fluctuations is weak (< 1 meV) and characteristic lateral regions differing by one ML are larger (30 – 40 nm) than the excitonic complex size (Bohr radius of order 10 nm). At the effective carrier temperatures of the experiment, most excitonic complexes are not localized and thus not describable by a simple harmonic potential (in which all states are localized). Nevertheless, the translational symmetry is broken and this can lead to experimental consequences, since the strict selection rules are relaxed. For the ODR experiments, constant FIR photon energy with the magnetic field varied, one therefore expects to observe a weak bound-to-bound transition, labeled T_b in Fig. 1(b), which occurs at a magnetic field *above* eCR (cf. inset of Fig. 2).

Figure 2 shows the dependence of all observed transitions on FIR photon energy; the various laser photon energies are indicated by dashed horizontal lines. The black solid line is the calculated position of free electron CR for the average QW width in which non-parabolicity is included with a two-band $\vec{k} \cdot \vec{p}$ model.^{22, 23} Numerical calculations of the positions of the onsets of the bound-to-continuum transitions for a “smooth” 20 nm GaAs/AlGaAs QW⁴ are shown as crossed circles; the dashed lines are guides to the eye. The field position of the bound-to-continuum transitions are difficult to determine experimentally for the two lowest FIR photon energies because they become increasingly broad and weak⁴, leading to the large error bars. This is also true for transition T_b , since the X^- -triplet becomes unbound at low-magnetic fields.²⁴ Theoretically, the precise position of a weakly allowed T_b transition is difficult to establish unambiguously at low magnetic fields. Strictly speaking, it becomes a resonance because the final bound triplet X^- in the first electron LL $n_e = 1$ merges with the continuum of states in the zeroth electron LL $n_e = 0$ (and, less importantly, with the continua of hole LLs $n_h > 1$). This leads to magnetic-field-dependent additional energy shifts and redistribution of the oscillator

strength (Fano resonance). These effects are very difficult to study in finite-size numerical calculations even with relatively large (6×10^3) Hamiltonian matrices involved. Although we have carried out such calculations, the interpretation of the calculated spectra is ambiguous. More importantly however, the parabolic model used to investigate the effects of lateral confinement theoretically, does not reflect the experimental conditions of very weak confinement that does not lead to full localization at the given temperatures.

Figure 3 shows ODR field scans at several temperatures at $E_{\text{FIR}} = 10.43$ meV for both sample 1²⁵ (Fig. 3(a)) and sample 2 (Fig. 3(b)). Both samples show the same bound-to-continuum transitions although the relative strengths are considerably different, due to a strong dependence on electron density⁴ and experimental conditions. More important, however, is the absence of any high-field shoulder above eCR for sample 1, which has no growth interrupts. In this case, the short range potential fluctuations due to well width fluctuations are very small (≈ 0.3 meV), and are further reduced significantly by the effective averaging of the exciton complex's relative motion.²⁶ Therefore, magnetic translational invariance is not affected strongly enough to allow observable bound-to-bound triplet transitions. In contrast, intentionally introduced random well-width fluctuations in sample 2, due to their long range, are sensed by the excitonic complex at low temperature, relaxing the strict selection rule and permitting the bound-to-bound transition T_b to be observed. The latter quickly disappears above $T = 15$ K, while the bound-to-continuum X^- -triplet transition T_1 is still observed. This is consistent with the excitonic complex being insensitive to the (weak) lateral potential fluctuations when the average thermal energy is larger than the energy amplitude of the fluctuations (0.75 meV), such that the X^- complex moves freely in the QW plane, i.e., the T_1 transition is a 2D bound to continuum

transitions and the triplet ground state lies slightly above the singlet ground states so that these transitions grow slightly in strength as temperature is increased and disappear near 30 K.

In conclusion, we have observed and identified a bound-to-bound transition associated with the X⁻-triplet in wide QWs with growth interrupts at the interfaces, which is strictly forbidden and not observed in translationally invariant systems. The weak confinement breaks magnetic translational invariance without fully localizing excitonic complexes at the temperatures investigated. This technique can be used to determine the degree of X⁻ localization in various samples and elucidate the origin of the oscillator strength of the so-called dark triplet state²⁷⁻³⁰ observed in photoluminescence experiments.

This research was supported in part by NSF-DMR # 0203560 and NSF-IGERT # DGE0114330. The work at CSUB was supported in part by a College Award of Cottrell Research Corporation. We are grateful to H. A. Nickel for use of the ODR data on sample 1.

References:

- *) On leave from General Physics Institute, RAS, Moscow 119991, Russia.
- ¹ A. B. Dzyubenko, JETP Lett. **66**, 617 (1997).
- ² H. A. Nickel, et al., Phys. Rev. B **62**, 2773 (2000).
- ³ A. B. Dzyubenko and A. Yu. Sivachenko, Phys. Rev. Lett. **84**, 4429 (2000).
- ⁴ H. A. Nickel, et al., Phys. Rev. Lett. **88**, 056801 (2002).
- ⁵ A. B. Dzyubenko and A. Yu. Sivachenko, Phys. Rev. B **48**, 14690 (1993).
- ⁶ Z. X. Jiang, et al., Phys. Rev. B **56**, R1692 (1997).
- ⁷ A. B. Dzyubenko and A. Yu. Sivachenko, Physica E **6**, 226 (2000).
- ⁸ J. Kono, et al., Phys. Rev. B **52**, R8654 (1995).
- ⁹ C. J. Meining, et al., Acta Phys. Pol. A **106**, 383 (2004).
- ¹⁰ C. J. Meining, et al., Physica E **26**, 158 (2005).
- ¹¹ B. N. Murdin, et al., Phys. Rev. B **62**, R7755 (2000).
- ¹² R. A. Child, et al., Phys. Rev. B **68**, 165307 (2003).
- ¹³ G. Eytan, et al., Phys. Rev. Lett. **81**, 1666 (1998).
- ¹⁴ D. Sanvitto, et al., Science **294**, 837 (2001).
- ¹⁵ D. Gammon, et al., Phys. Rev. Lett. **67**, 1547 (1991).
- ¹⁶ K. Leosson, et al., Phys. Rev. B **61**, 10322 (2000).
- ¹⁷ J. G. Tischler, et al., Phys. Rev. B **66**, 081310(R) (2002).
- ¹⁸ D. Gammon, et al., Phys. Rev. Lett. **76**, 3005 (1996).
- ¹⁹ D. Gammon, et al., Science **273**, 87 (1996).
- ²⁰ G. Kioseoglou, et al., Phys. Rev. B **61**, 4780 (2000).
- ²¹ I. Vurgaftman, et al., J. Appl. Phys. **89**, 5815 (2001).

²² W. Zawadzki, J. Phys. C **16**, 229 (1983).

²³ W. Seidenbusch, et al., Surf. Sci. **142**, 375 (1984).

²⁴ T. Vanhoucke, et al., Phys. Rev. B **65**, 233305 (2002).

²⁵ H. A. Nickel, Dissertation, University at Buffalo, 2000.

²⁶ E. Runge, in *Solid State Physics*, edited by H. Ehrenreich and F. Spaepen (Academic Press, Amsterdam, 2002), Vol. 57, p. 149.

²⁷ D. Sanvitto, et al., Phys. Rev. Lett. **89**, 246805 (2002).

²⁸ C. Schüller, et al., Phys. Rev. B, **65**, 081301(R) (2002).

²⁹ B. M. Ashkinadze, et al., Phys. Rev. B **69**, 115303 (2004).

³⁰ G. V. Astakhov, et al., Phys. Rev. B **71**, 201312(R) (2005).

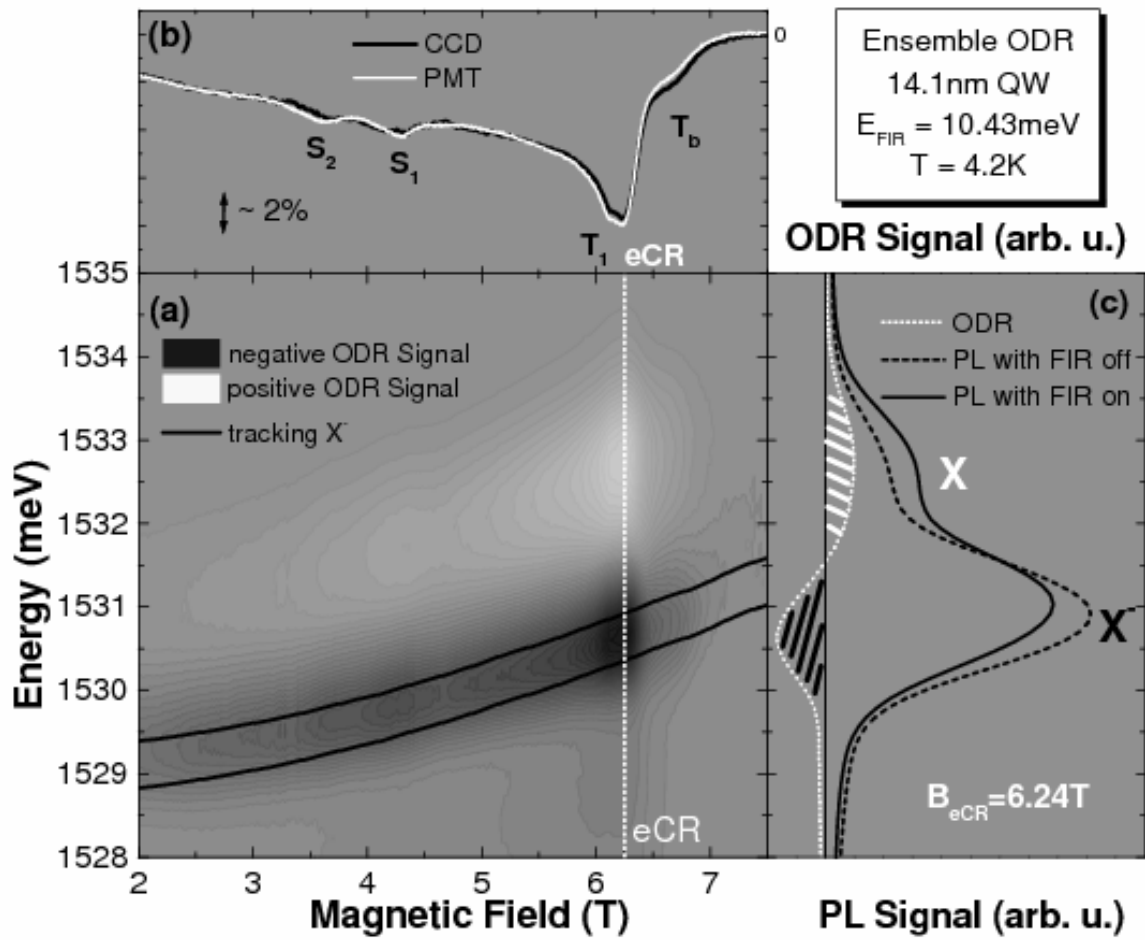


Fig. 1: *C. J. Meining et al.*, Phys. Rev. B

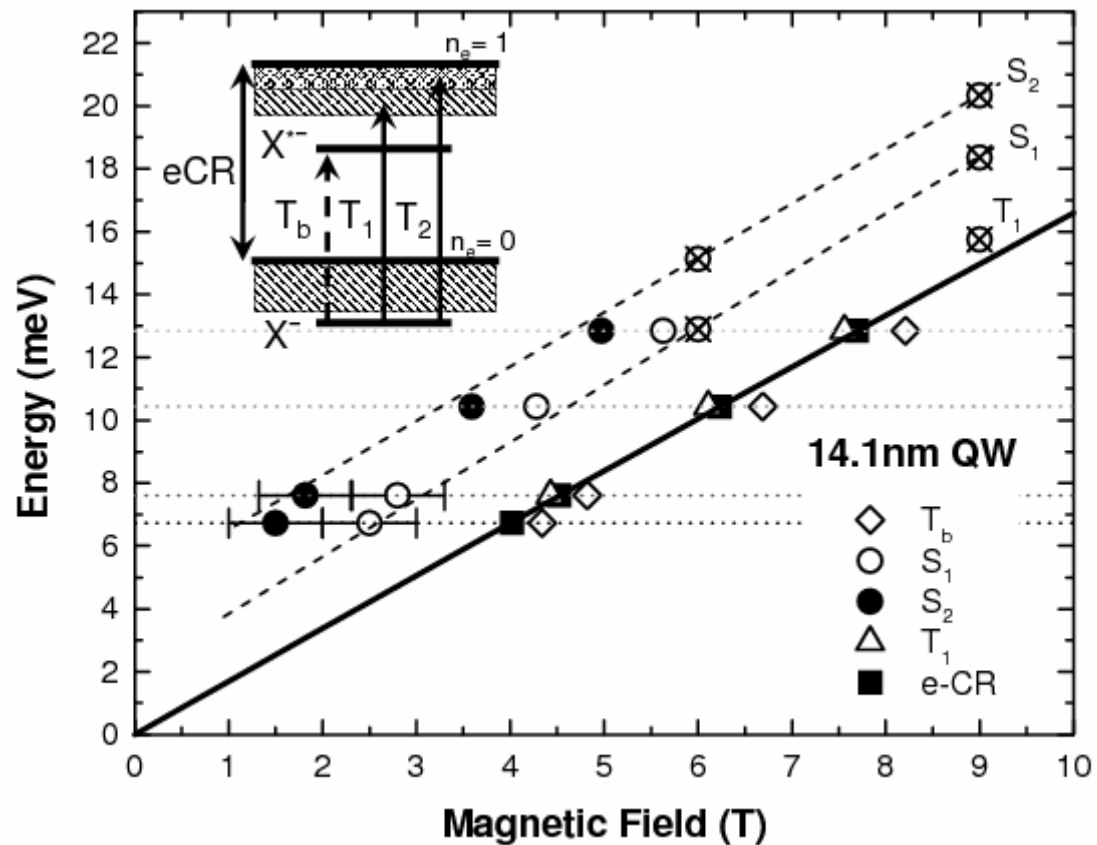


Fig. 2: C. J. Meining *et al.*, Phys. Rev. B

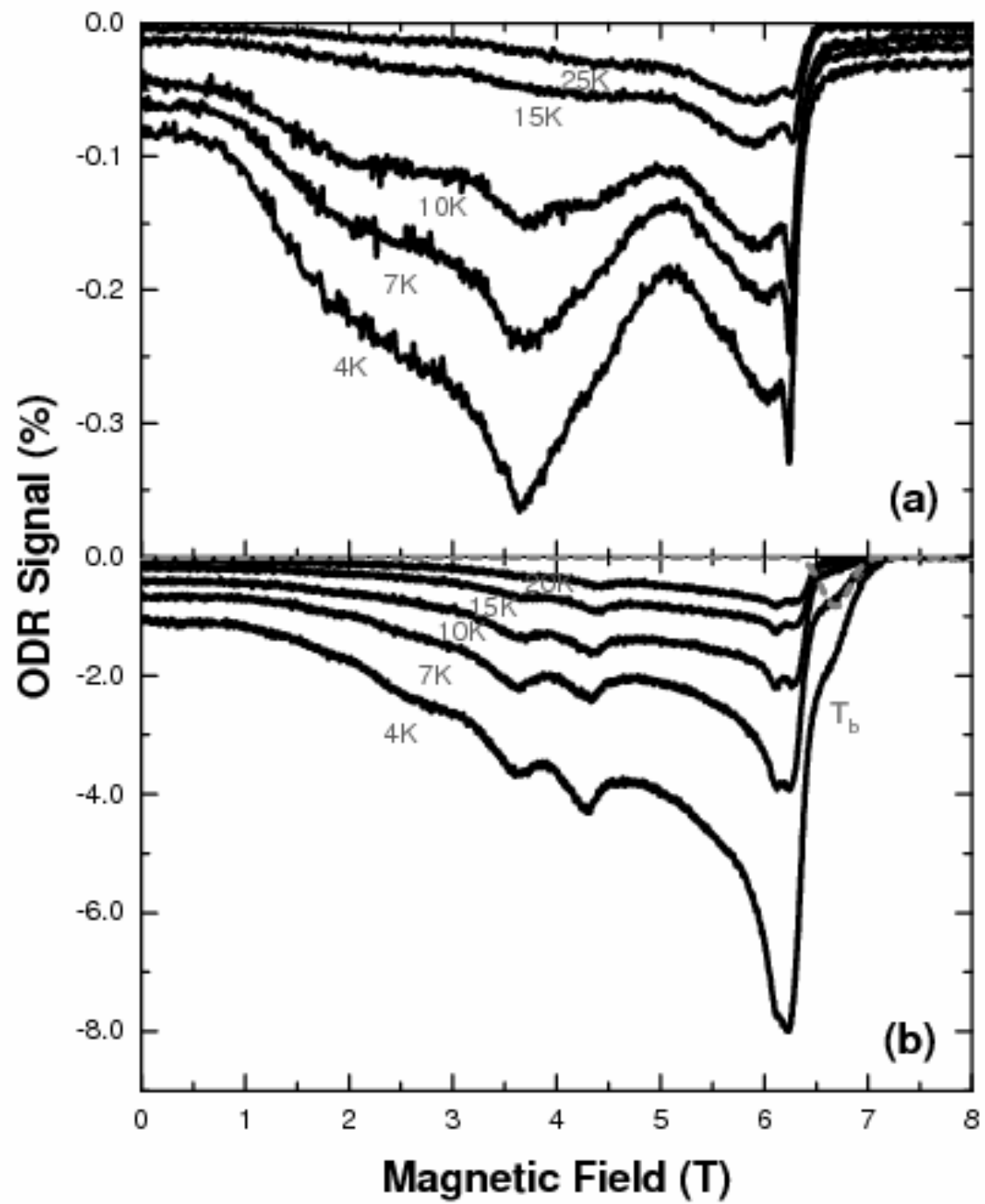


Fig. 3: *C. J. Meining et al., Phys. Rev. B*

Figure Captions:

Fig. 1: ODR of a 14.1 nm wide QW at $E_{\text{FIR}} = 10.43$ meV with PMT and CCD detection. **(a)** Gray scale contour plot of the CCD-ODR signal. Dark (bright) regions corresponds to negative (positive) ODR signal. **(b)** ODR field scans obtained with CCD (thick black line) and PMT detection (thin white line). The bandpass used is indicated in (a) by the pair of thick black lines. Bound-to-continuum internal transitions of the X^- -singlet (S_1, S_2), the X^- -triplet (T_1), electron cyclotron resonance (eCR), and a bound-to-bound internal transition associated with the X^- -triplet (T_b) are observed. **(c)** ODR energy scan (dotted white line) and CCD-PL with FIR laser on (solid black) and off (dashed black) at $B = 6.24$ T (the position of eCR is indicated by the vertical white dotted line in (a)).

Fig. 2: Dependence of the observed transitions of sample 2 (14.1 nm QW; cf. Fig. 1(b)) on FIR photon energy; eCR (squares), bound-to-continuum internal transitions of the X^- -singlet (circles), the X^- -triplet (triangles), and an additional bound-to-bound, internal X^- -triplet transition (diamonds) are indicated. Solid black line: calculated eCR including non-parabolicity via a two-band model. Dotted horizontal lines indicate the FIR photon energy. The crossed circles mark the numerical calculations at 6 T and 9 T for 20 nm QWs without lateral confinement; straight dashed lines are guides to the eye. Inset: schematic of the initial and final states of the X^- -triplet and relevant FIR transitions associated with the two lowest electron LLs.

Fig. 3: Temperature study of the ODR signal for samples 1 **(a)** and 2 **(b)** for $E_{\text{FIR}} = 10.43$ meV. In both panels the signal decreases with increasing temperature. Note the clear feature above eCR for sample 2 as indicated by the dashed gray line obtained by fitting and subtracting the contributions below eCR at 4.2 K.